catalysts

MDPI

Communication

Solvent Effect in Catalytic Lignin Hydrogenolysis

Dennis Panke, German Bechthold and Thomas E. Müller *

Carbon Sources and Conversion, Faculty of Mechanical Engineering, Ruhr-Universität Bochum, Universitätsstr. 150, 44801 Bochum, Germany; dennis.panke@ls-csc.ruhr-uni-bochum.de (D.P.); german.bechthold@ruhr-uni-bochum.de (G.B.)
* Correspondence: mueller@ls-csc.rub.de; Tel.: +49-234-32-26390

Abstract: The solvent effect in the catalytic depolymerization of the three-dimensional network of lignin is discussed based on recent reports in this field. Also, the results of an experimental study on the depolymerization of kraft lignin are presented. The cleavage of ether bonds within the lignin network was promoted using ruthenium and platinum on activated carbon (Ru/C and Pt/C), two common hydrogenolysis catalysts. Methanol was identified as a suitable solvent. Noteworthy, under the chosen reaction conditions, the catalysts showed significant resilience to the sulfur present in kraft lignin. The conversion of kraft lignin to lignin oil was strongly affected by the reaction conditions. Although the Ru/C catalyst provided the highest yield at supercritical conditions, a maximum yield was obtained for the Pt/C catalyst at near-critical conditions. The formation of guaiacol, 4-alkylguaiacols, isoeugenol, and 4-ethyl-2,6-dimethoxyphenol is attributed to the solubility of oligomeric lignin fragments in the solvent and the relative propensity of specific groups to adsorb on the catalyst surface.

Keywords: lignin; aromatics; solvent effect; hydrogenolysis; hydrogenation; hydrogen; ruthenium catalyst; platinum catalyst; sustainability

Citation: Panke, D.; Bechthold, G.; Müller, T.E. Solvent Effect in Catalytic Lignin Hydrogenolysis. *Catalysts* **2022**, *12*, 664. https://doi.org/10.3390/catal12060664

Academic Editor: Laurent Djakovitch

Received: 14 April 2022
Accepted: 11 June 2022
Published: 17 June 2022

1. Introduction

Myriad industrial production chains still rely upon fossil resources for manufacturing polymers, platform chemicals, and fuels [1]. To counter this dependency and promote more environmentally, politically, and economically sustainable supply chains, research is increasingly focused on exploiting renewable resources as a viable alternative [1]. Certain fractions of biomass, an important class of renewables, comprise aromatic entities that can be exploited as chemical feedstock and for industrial applications [2].

In nature, aromatic structures are found in various organic structures, such as plant dyes [3], hormones [4], phenolic phytochemicals [5], and lignin [6,7]. The biopolymer lignin is the largest natural resource that contains aromatics as a structural element. The overall amount of lignin in the biosphere is estimated to be 300 billion t [8]. A significant fraction of the carbon that is bound by photosynthesis in terrestrial and oceanic primary production (56.4 billion t/a and 48.5 billion t/a, respectively [9]) is converted to lignin. The annual increase is estimated at 20 billion t/a [9], which corresponds to about 11–13% of the annual biomass generation of 150–180 billion t/a [9] by photosynthesis.

At pulp and paper facilities, 50–70 million tons of lignin are produced annually as a by-product [9]. Major fractions of this lignin are obtained as lignosulfonate (88%) and kraft lignin (9%) [9]. Organosolv lignin currently accounts for 2% of the production and is expected to grow to 225 million t/a by 2030 [9] as a result of second-generation biofuel generation. In contrast, the anthropogenic utilization of aromatic compounds comprises 264 million t of benzene, toluene, and xylenes (BTX) annually [2]. As it is abundant worldwide, lignin is a promising raw material to replace those derived from fossil resources.

Together with cellulose and hemicellulose, lignin forms a structural key element of the cell walls of vascular plants. The lignin scaffold protects the cell from external influences such as the penetration of water, chemical compounds, and pests. It also increases the compressive strength of the cells and gives rise to the hydrophobic environment of the vascular bundle effective for water transport [10]. Depending on the species of vegetation, lignin constitutes up to 15–40% of the dry plant matter [11]. The lignin content in the cell wall considerably on the type of plant. Three plant categories, softwoods (25–30% lignin), hardwoods (22–27% lignin), and grass plants (1–19% lignin) are commonly distinguished [12,13]. Robust parts of plants, such as wood, contain higher levels of lignin than leaf stalks or flowers.

The structure of lignin is derived from three monolignol building blocks: coumaryl alcohol (commonly referred to as building block H), coniferyl alcohol (building block G), and sinapyl alcohol (building block S), all of which are defined by the presence of an aromatic ring in the structure (Scheme 1). In nature, the biosynthesis of monolignol branches occurs via the phenylpropanoid pathway [10]. The structural entities differ in the number of linkages and the number of hydroxy and methoxy substituents. Other phenolic compounds, such as flavonoids, hydroxystilbenes, and hydroxycinnamic amides, can also be incorporated into the structure of lignin [14]. Once synthesized, the monomers are transported to the cell wall where they are oxidized in the presence of peroxidases and/or laccases to form the corresponding radicals [14]. In a largely chemically controlled reaction sequence, polymerization occurs through free-radical coupling [14]. As a result, the monomeric building blocks are attached in a combinatorial fashion to the growing three-dimensional structure. Through the stepwise radical reaction sequence, various ether bonds (C-O-C) and carbon–carbon bonds (C–C) are generated that differ from each other regarding their bond-dissociation energies (BDE). Once the growth of the network has ended, the three-dimensional structure of lignin reflects a multifaceted biopolymer [12,15].

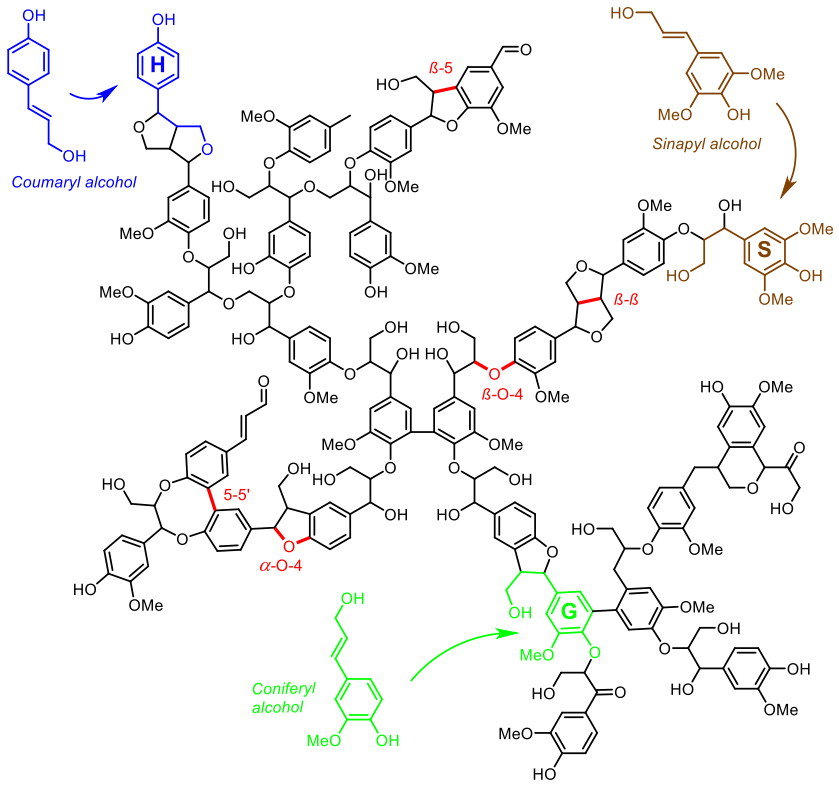

Scheme 1. Typical part of the structure of lignin. Basic building blocks, sinapyl alcohol (M = 210.23 g/mol), coniferyl alcohol (M = 180.20 g/mol), and coumaryl alcohol (M = 150.18 g/mol), and selected bond types are highlighted; simplified structure of lignin, see also [16].

Different types of wood are characterized by different distributions of the monolignol building blocks. Table 1 gives an overview of these various distributions.

Table 1. Relative content of building blocks that constitute lignin. Data are summarized from references [12,17,18].

Building Block	Hardwood [%]	Softwood [%]
H	0–8	5
G	25–50	95
S	54–75	0

Moreover, Table 2 shows an overview of the bond types in lignin. Hereby, aryl ether linkages, ß-O-4 and α-O-4, predominate, constituting 49–73% of the lignin bonds in hardwoods and 48–62% in conifers [12,17,18]. The diversity of the bonds renders lignin with high resilience to degradation through cleavage of chemical bonds.

Table 2. Overview of the bond types occurring in lignin listed in the order of increasing bond dissociation energies. Data are summarized from references [12,17,18].

Bond Type	Hardwood [%]	Softwood [%]	BDE [kJ/mol]
α-O-4	4–8	6–12	222
ß-1 (C-C)	5–7	3–10	285
β-O-4	45–65	42–50	313
4-O-5	6–7	3.5–8	335
5-5	4–10	9.5–25	481
ß-5	3–11	9–12	523
ß-1 (C=C)	minor	minor	690

BDE, bond dissociation energy.

To make lignin accessible for industrial processing, the molecule first needs to be separated from cellulose and hemicellulose. Various processes have been commercialized to do this [9,11,19]. These include treating the lignocellulosic raw material with acids (sulfite process), alkali (kraft process, [20]), enzymes (soda process), or organic solvents (organosolv process). All these processes change the basic structure of lignin by cleavage of the aryl ether bonds. Up to 86% of the *β-O-4* and *α-O-4* ether bonds are replaced by condensed carbon–carbon bonds during the repolymerization reactions of the resulting lignin fragments [17]. Since these have higher bond-dissociation energies (BDE, Table 2), the energy expenditure for downstream depolymerization processes is correspondingly higher.

The kraft process, also known as the sulfide process, is mostly used in the manufacture of paper and yields 50 million tons of kraft lignin annually [13]. During this process, crushed biomass (wood chips, straw, bagasse, and other lignin-rich biomasses) is boiled in a white liquor solution of caustic soda and sodium sulfide at 140 to 170 °C and 7 to 10 bar pressure for several hours. By nucleophilic substitution, the lignin is cleaved by sulfide anions. The cellulose is separated from the cell wall structure and removed. The remaining mixture of dissolved lignin, chemicals from the white liquor, and degradation products from the hemicellulose, is commonly referred to as black liquor. Typically, the black liquor is burned to generate energy and recover some of the chemical components [21]. In an alternative process, referred to as the LignoBoost process, the lignin is precipitated by lowering the pH value through acidification with sulfuric acid or carbon dioxide [22]. Additionally, the subsequent treatment of the raw kraft lignin with sodium hydroxide reduces the sulfur content in the final product [17]. The residual sulfur content hampers subsequent chemical processing because sulfur compounds act as potent poisons for metal-based and Lewis acidic catalysts.

Depending on the composition of the biomass and the process conditions, the lignin obtained in the industrial kraft process comprises a diverse mixture of lignin molecules that differ widely in structure, by-products (mostly soluble carbohydrates), and inorganic

components (including sulfur compounds). Furthermore, as a result of the repolymerization reactions, the lignin molecules often have a higher molar mass than the compounds initially released from the native lignin. Kraft lignin tends to be marked by a pronounced fraction of condensed C–C bonds that link the aromatic fragments. Table 3 depicts the typical composition of kraft lignin.

Table 3. Typical composition of kraft lignin. Data are summarized from references [17,23].

Descriptor	Value	Unit
Molar mass	1500–5000 [1]	[g/mol]
Polydispersity	2.5–3.5	[-]
Acid-soluble lignin fraction	1–4.9	[wt.-%]
Carbohydrate fraction	1–2.3	[wt.-%]
Water content (often referred to as humidity)	3–6	[wt.-%]
Nitrogen content	0.05	[wt.-%]
Sulfur content	1.8	[wt.-%]
Incombustible residue (ash)	0.5–3	[wt.-%]

[1] up to 25,000 g/mol.

This study concerns the solvent effect in the catalytic depolymerization of kraft lignin. The conditions under which the ruthenium and platinum on activated carbon (Ru/C and Pt/C) are suitable catalysts that also work in the presence of residual sulfur compounds present in kraft lignin were also explored. The concurrent hydrogenation of unsaturated groups in the cleavage products was targeted at obtaining lignin oils with significant shelf life and the aromatic groups of kraft lignin were supposed to remain intact. It was shown that with methanol as solvent and reaction conditions close to the supercritical point of methanol, kraft lignin can be converted to a lignin oil comprising guaiacol, 4-alkylguaiacols, isoeugenol, and 4-ethyl-2,6-dimethoxyphenol.

2. Solvent Effect in Lignin Depolymerization

2.1. Hydrogenolysis

In the hydrogenolysis of lignin, the ether bonds (*ß-O-4* and *α-O-4*) are cleaved at temperatures of 200–250 °C. Using catalysts is essential here, especially because the specific lignin-derived target molecules need to be generated at high yields and minimal costs regarding the downstream separation of the usually broad product spectrum [24–26]. Typical catalyst base metals are platinum, ruthenium, palladium, and rhodium, which are applied as nanoparticles supported on activated carbon, which has a high surface area [27]. In studies with platinum on activated carbon (Pt/C) and ruthenium on activated carbon (Ru/C), various results were obtained concerning the yield and composition of the lignin oil obtained. According to Kristianto et al. (2017), using a Ru/C catalyst in an ethanol solution increased the yield of lignin oil by 11 wt.-% to 42 wt.-% [18,28]. Moreover, Yan et al. (2008) found an increase in the yield of mononuclear aromatics of 29% when Ru/C was replaced by Pt/C [29]. In further investigations, ruthenium provided higher selectivity for the conversion of lignin to the cleavage products guaiacol and 4-ethylphenol [30–32].

2.2. Choice of Solvent

Choosing the optimal solvent is very important in obtaining high yields in the depolymerization of lignin. Being an inhomogeneous biopolymer comprising nonpolar aliphatic and aromatic groups as well as highly polar hetero-functional entities, lignin shows low solubility in many solvents. Native lignin is also characterized by a three-dimensional network of linkages (see also Scheme 1) that renders it insoluble.

Depending on the isolation process, the processed starting materials differ widely in solubility. Technical-grade lignin typically has very low solubility in water and organic solvents such as ethanol, acetone, 1,4-dioxane, and the corresponding two-component mixtures [33]. Nevertheless, the solubility increases with increasing temperature. Zakzeski et al.

(2012) showed that the solubility of organosolv and kraft lignins in a 1:1 mixture of water and ethanol increases strongly with the solvent temperature, whereby complete solubility is obtained at 115 °C and 225 °C, respectively [33].

The availability of hydrogen is frequently a limiting factor in hydrogenolysis reactions. As hydrogen has limited solubility in many reaction media, it is important to avoid mass transfer limitations for introducing hydrogen from the gas phase into the reaction medium, thereby accelerating hydrogenolysis and hydrogenation reactions. Since unsaturated intermediates are converted rapidly in the presence of ample amounts of hydrogen, the propensity for repolymerization is reduced. For example, Shu et al. (2016) showed that with increasing availability of hydrogen, repolymerization reactions to solid residues were reduced and higher oil yields were obtained simultaneously [34]. By applying supercritical media mass transfer limitations can be reduced skirting the potentially slow transfer of hydrogen from the gas phase to the liquid phase (*vide infra*).

The solvent used in the depolymerization of lignin can also take part in the course of the reaction. Important roles are played by the transesterification reactions and the provision of hydrogen for in situ transfer-hydrogenolysis reactions [35]. In addition to reacting with lignin, the solvent can also undergo reactions with itself. By using an α-molybdenum carbide catalyst in ethanol, for instance, Ma et al. (2014) obtained a lignin-oil yield 60% higher than the mass of the introduced kraft lignin [36]. Consequently, a reaction comprising the solvent must have taken place; this needs to be taken into account from an economic perspective and weighed against possible advantages.

2.3. Supercritical Fluids

Fluids close to their critical point are particularly interesting as solvents. Once the critical temperature (T_C) and critical pressure (p_C) have been exceeded, distinct liquid and gas phases do not exist. Supercritical fluids assume physical properties of gaseous and liquid states alike [37]. The respective fluid properties change drastically upon exceeding the critical point. When chosen correctly, the advantages of liquid and gaseous media can be exploited. Thus, an increase in pressure beyond the critical point leads to a significant increase in the density of gases and, consequently, increased solubilizing power. Diffusion rates in supercritical fluids are higher than in classic liquid solvents. In a mono-phase system, this leads to high availability of hydrogen. In a biphasic system, the diffusion rate of the hydrogen molecules into the more dense phase containing the lignin is increased close to the critical point [38]. Furthermore, the substance transport of the reactants into larger three-dimensional lignin fragments as well as catalyst pores, in the case of a heterogeneous catalyst, is promoted through the lower viscosity and density of the surrounding medium. This combination of properties renders fluids close to the critical point as interesting solvents for the processing of lignin.

Figure 1 presents a summary of the various critical points of the common solvents [39–41]. Alcohols provide readily accessible critical points. In the series of alcohols, the shortest homolog methanol has the highest polarity, whereby the polarity as solvent decreases with the chain length. Thus, in this series, methanol generally provides the best solubility for lignin. In contrast, even though water is more polar, it is characterized by critical points at much higher temperatures and pressures. Also, water close to or above the critical point tends to be highly corrosive. In comparison, the critical point of ammonia is reached more readily. Even so, ammonia tends to react with unsaturated groups in lignin and the desired target products. Consequently, the use of ammonia has not been studied intensively so far. In comparison, the critical points of carbon dioxide and alkanes are reached at relatively low temperatures and pressures. However, the solubilizing power of carbon dioxide and alkanes is typical for non-polar solvents and due to the low solubility of the starting material, these solvents are less suitable for lignin conversion.

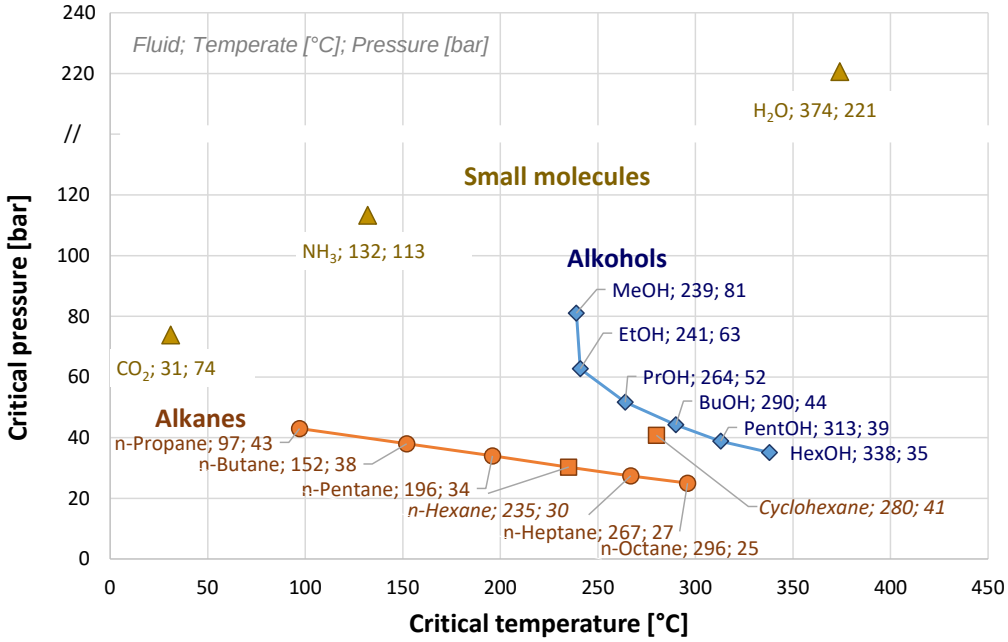

Figure 1. Critical point of common solvents. Numbers stated after the name of the solvent refer to the critical temperature [°C] and pressure [bar], respectively.

2.4. Examples of Lignin Conversion in Near-Critical or Supercritical Fluids

Supercritical methanol was shown to provide a good compromise with regard to the solvent's dissolution power, diffusivity, and acid-base properties [42]. The yield in mononuclear products in a reaction that was performed at 300 °C and a starting pressure of 20 bar was enhanced significantly upon employing a Pd/C hydrogenation catalyst [42]. However, it was found that the ß-O-4 linkages were cleaved to a considerable extent and repolymerization occurred mostly through the formation of ß–ß linkages. Likewise, the use of an acid-base catalyst ($S_2O_8^{2-}$/KNO_3/TiO_2) in combination with a hydrogenation catalyst (Ru/C) produced an enhanced yield for mononuclear and dinuclear aromatic products by using a mixture of 1,4-dioxane and methanol (320 °C, 40 bar before heating, 6 h) [43].

Supercritical ethanol was found to provide more effective processing of lignin than water [44]. In ethanol, the formation of phenol, guaiacol, and alkylguaiacols was enhanced, whereas aqueous mixtures yielded more catechol [45]. Yields in lignin oil of more than 80 wt.-% could be achieved [46]. Upon using ethanol, Kim et al. (2013) reported a lignin-oil yield of 91.7% that was obtained at a reaction temperature of 200 °C [47]. In a mixture of ethanol and water, the molecular weight M_n of lignin could be reduced from 10,000 g·mol^{-1} to 415 g·mol^{-1} at a reaction temperature of 300 °C and within 2 h [48]. At lower temperatures, the lignin ether bonds were not cleaved, whereas applying higher temperatures led to recondensation reactions and increased char formation.

The use of near-critical water was optimized for the conversion of LignoBoost kraft lignin over ZrO_2 [49]. The reaction was performed in a stirred tank reactor with recycle. The reaction temperature of 350 °C and 250 bar related to a density of water of 625 kg·m^{-3}. At these conditions, a higher retention of aromatic rings was observed compared to the stronger conditions that were employed before. At a residence time of 11 min, a mixture of phenolic compounds and a bio-oil was obtained. In the water-soluble fraction, cresols, guaiacols, and catechols were identified as the predominant mononuclear aromatic compounds generated. The yield of mononuclear aromatic compounds increased substantially when using K_2CO_3 as a co-catalyst with a remarkable increase in the yield of anisols and a moderate increase in the yield of alkylphenols and catechols.

3. Cleavage of Lignin by Hydrogenolysis

In an experimental study, we explored the effects of the physical state of the solvent on the depolymerization of kraft lignin. The aim was to cleave the aromatic ether bonds of the lignin network by hydrogenolysis with molecular hydrogen and to simultaneously hydrogenate any unsaturated groups that may have formed. Aromatic moieties were supposed to stay untouched. As hydrogenolysis catalysts are known to have a high propensity for ether cleavage, ruthenium on activated carbon (Ru/C, 5 wt.-%) as well as platinum on activated carbon (Pt/C, 10 wt.-%) were used. We anticipated these catalysts to show certain tolerance to the sulfur compounds present in kraft lignin.

3.1. Lignin Depolymerization in Methanol

Methanol was chosen as the solvent for further experiments because of its good solubilizing power, well-accessible critical point (Tc 239 °C, pc 81 bar), and high solubility for molecular hydrogen compared to many other polar solvents. In a parameter study, the methanol was employed as a solvent at conditions below the critical point (200 °C, 76 bar, subcritical), conditions close to the critical point (235 °C, 110 bar, near-critical), and conditions above the critical point (250 °C, 131 bar, supercritical). For the reaction, kraft lignin and the catalyst were placed into a high-pressure reactor and heated under an atmosphere of hydrogen for 40 min to the reaction temperature. After the reactor was cooled and the volatiles were removed under partial vacuum, a viscous oil was obtained as the product.

Upon using Ru/C, a steady increase in the lignin-oil yield from 35% to 51% was observed with the reaction temperature (Figure 2). When Pt/C was used as the catalyst, the yields were somewhat higher in sub-critical conditions (46%) and near-critical conditions (62%). Upon further increasing the temperature, the yield decreased to 24%. In a reference experiment carried out at near-critical conditions but without the addition of a catalyst, a lignin-oil yield of 34% was obtained. Thus, the use of a catalyst leads to a substantial increase in the yield of lignin oil. The decrease in the yield observed for the Pt/C catalyst at supercritical conditions may indicate an increased tendency towards repolymerization of the lignin fragments.

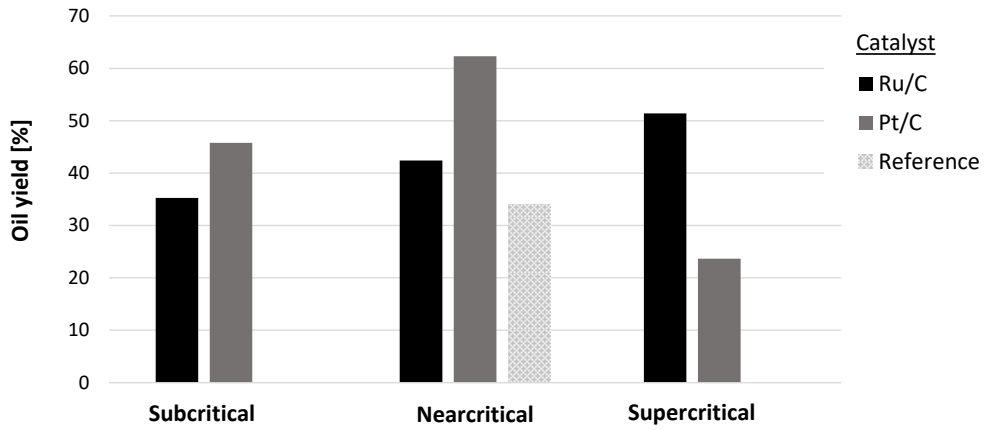

Figure 2. Yield in lignin oil obtained by catalytic hydrogenolysis of kraft lignin in methanol at subcritical (200 °C, 76 bar, **left**), near-critical (235 °C, 110 bar, **middle**), and supercritical (250 °C, 131 bar, **right**) conditions.

3.2. Product Spectrum of Lignin Depolymerization in Methanol

The lignin oil was then analyzed by gas chromatography–mass spectrometry (GC–MS). Various mononuclear guaiacol-type isomers were identified as the main products (Figure 3). Clearly visible are the series guaiacol, 4-methylguaiacol, 4-ethylguaiacol, and 4-propylguaiacol. Noteworthy is that the synthesis of isoeugenol showed much higher yields in the reference experiments than in the catalyzed reactions. This suggests that the side chain is hydrogenated in

the presence of the catalyst in a subsequent reaction that converts isoeugenol to 4-ethylguaiacol. At a longer retention time, 2,6-dimethoxy-4-hydroxyethyl-phenol or a corresponding isomer was observed. At even longer retention times, mostly polynuclear aromatic compounds of higher molecular weight were detected.

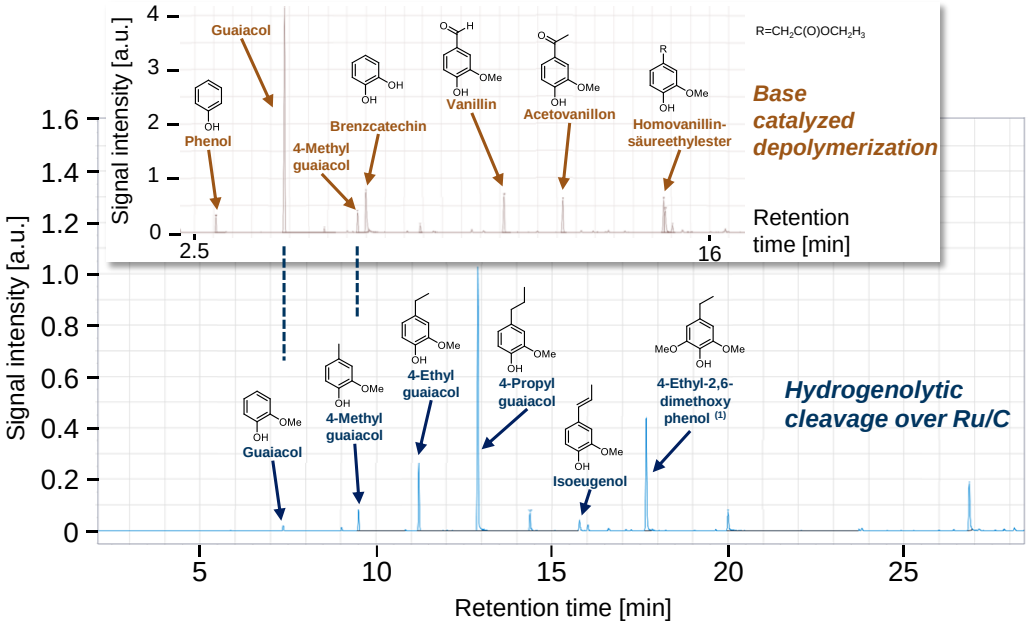

Figure 3. Typical gas chromatogram of lignin oil obtained by catalytic hydrogenolysis of kraft lignin in methanol (kraft lignin, Ru/C, 0.09 mmol Ru/g lignin, 30 bar H_2 at room temperature, 40 min) and assignment of the compounds (blue, (1) 4-ethyl-2,6-dimethoxyphenol or isomer) in comparison to the corresponding product mixture obtained by base-catalyzed depolymerization of kraft lignin (insert). Both chromatograms were measured on the same column and the scale was adjusted so that corresponding compounds match on the abscissa.

The product spectrum was compared to the corresponding base-catalyzed depolymerization of lignin (Figure 3, insert). Also here, a mixture of monomeric phenolic compounds was obtained but the product distribution was entirely different. In addition to phenol and guaiacol, vanillin and acetovanillone—which are highly susceptible to subsequent reactions due to the reactive carbonyl group—were also obtained. In contrast, the hydrogenolysis of lignin with Ru/C has a higher propensity to form α-methylether-substituted phenols, such as methyl-, ethyl- and propylguaiacol, and a much narrower product distribution than that obtained with base catalysis.

The relative yields in mononuclear aromatics obtained over Ru/C and Pt/C are depicted in Figures 4 and 5, respectively. Clearly, both catalysts, Ru/C and Pt/C, show a similar distribution of mononuclear aromatics. Moreover, the choice of the reaction conditions had little influence on the distribution. A slight increase in the yield of 4-ethylguaiacol is observed for Ru/C at near-critical conditions and for both catalysts under supercritical conditions.

Noteworthy is that the yield of 4-ethylguaiacol was also higher in the Ru/C- and Pt/C-catalyzed reaction compared to the uncatalyzed reference reaction. This is consistent with the hydrogenation of the double bond in the side-chain of the 4-vinylguaiacol molecule to 4-ethylguaiacol (Scheme 2, see also [50]). In turn, 4-vinylguaiacol was only found in the product spectrum of the uncatalyzed reference reaction, which supports the conclusion that at least some of the 4-ethylguaiacol is obtained by hydrogenation of the vinyl group of the corresponding 4-vinylguaiacol precursor. Similarly, hydrogenation of the 1-propenyl moiety in isoeugenol may contribute to the formation of 4-propylguaiacol in the reaction mixture.

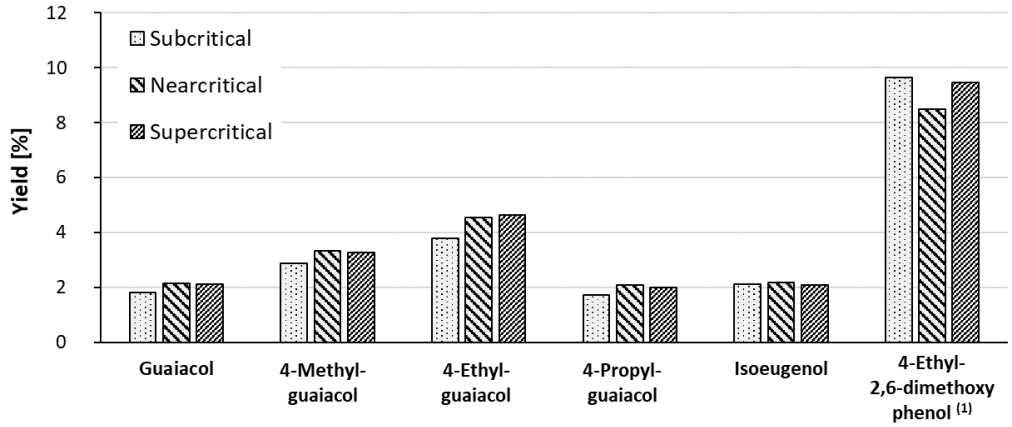

Figure 4. Mononuclear products observed for catalytic hydrogenolysis of kraft lignin in methanol with Ru/C at subcritical (200 °C, 76 bar, **left**), near-critical (235 °C, 110 bar, **middle**), and supercritical (250 °C, 131 bar, **right**) conditions; (1) 4-ethyl-2,6-dimethoxyphenol or isomer.

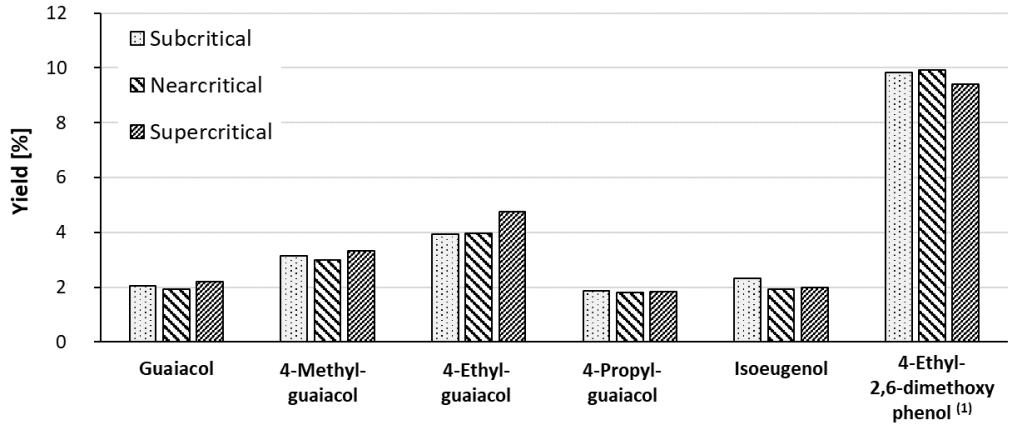

Figure 5. Mononuclear products observed for catalytic hydrogenolysis of kraft lignin in methanol with Pt/C at subcritical (200 °C, 76 bar, **left**), near-critical (235 °C, 110 bar, **middle**), and supercritical (250 °C, 131 bar, **right**) conditions; (1) 4-ethyl-2,6-dimethoxyphenol or isomer.

Scheme 2. Likely step in the reaction sequence by hydrogenation of the vinylic moieties of isoeugenol to 4-propylguaiacol (**left**) and of 4-vinylguaiacol to 4-ethylguaiacol (**right**).

Thus, the formation of guaiacol, 4-alkylguaiacols, isoeugenol, and 4-ethyl-2,6-dimethox yphenol or its isomers is consistent with a gradual dissolution of oligomeric lignin fragments in the methanol. The product distribution is consistent with the presence of sinapyl alcohol and coniferyl alcohol, which are the dominant building blocks (S and G, respectively) in the parent lignin. A comparison of the product spectrum suggests that the aromatic moieties have an adequate propensity to adsorb onto the catalyst surface for the hydrogenolysis reaction to proceed. Moreover, the vinylic entities in the mononuclear aromatic must be able to adsorb onto the catalyst surface as a prerequisite for their hydrogenation to the corresponding aliphatic side chain. Please note that the aromatic moieties are retained throughout the catalytic reaction. This suggests that the aromatic rings have a sufficiently low propensity to adsorb on the catalyst surface and, thus, remain

untouched. This opens new avenues for the production of aromatic compounds from kraft lignin through site-specific selective catalytic conversion.

3.3. Hydrogenolytic Cleavage of Aryl Ether Moieties in Lignin Depolymerization

Finally, the chemical transformations occurring during the depolymerization of lignin were explored. The characterization of the parent kraft lignin by solid-state NMR spectroscopy is hampered by the large variety of chemical entities in lignin and the intrinsically low natural abundance of ^{13}C nuclei. For enhancing the signal intensity, we turned to dynamic nuclear polarization (DNP)-enhanced ^{13}C-NMR spectroscopy. A comparison between the ^{13}C-DNP-NMR spectrum and a conventional ^{13}-C-MAS-NMR spectrum of kraft lignin is shown in Figure 6. Clearly, the signal intensity is greatly enhanced upon using DNP. Signals assigned to the aromatic moieties, the electron-deficient CH/CH_2-groups that are located in the vicinity of oxygen atoms, and the aliphatic methoxy groups are clearly observed. Noteworthy is the enhanced intensity of the signals assigned to the CH/CH_2-moieties.

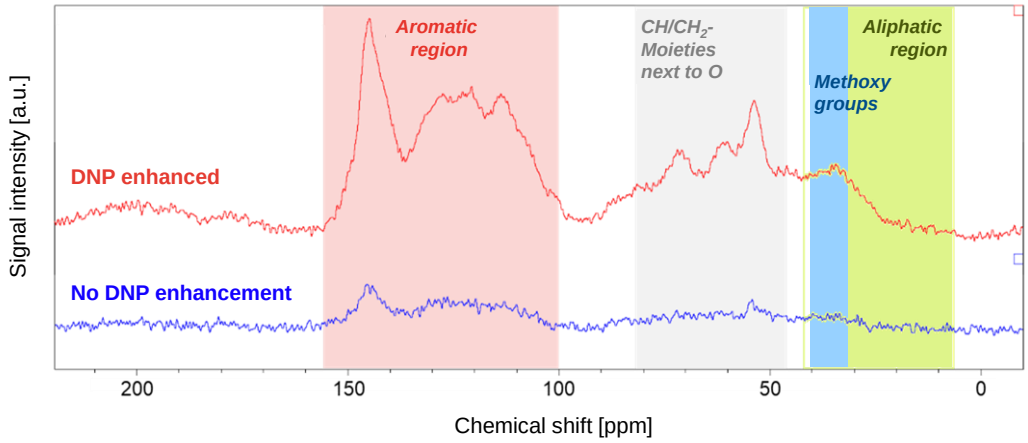

Figure 6. ^{1}H-^{13}C CP-MAS spectra of kraft lignin recorded with DNP enhancement (red, **top**) and without DNP enhancement (blue, **bottom**); spectra were recorded with the same number of scans (512 scans).

In the next step, the phase-sensitive heteronuclear single quantum coherence NMR spectra (^{1}H,^{13}C-HSQC-NMR) of the parent kraft lignin (Figure 7, blue and green) and of the lignin oil obtained by the hydrogenolysis of kraft lignin (Figure 7, red and pink) were compared. This pulse sequence is used to correlate the ^{1}H chemical shift with the ^{13}C chemical shift. Observed are the directly bonded hydrogen–carbon moieties via their $^{1}J_{CH}$ coupling. A useful feature is that the carbons bearing an even (CH_2) or odd number (CH or CH_3) of hydrogen atoms are differentiated. This difference is encoded into the sign of the correlation peak and shown in the respective color. The HSQC NMR spectra of the lignin oils obtained by hydrogenolysis of kraft lignin over Ru/C (Figure 7) and Pt/C (Figure S1) were essentially identical.

Correlation signals are clearly observed in the aromatic region, the electron-deficient CH/CH_2-groups that are located in the vicinity of oxygen atoms, the methoxy groups, and the aliphatic $CH/CH_2/CH_3$ groups (Figure 7). There are substantial differences in the correlation spectra of the parent kraft lignin and the lignin oil. Thus, the reduced intensity of deshielded aromatic CH groups, assigned to electron-rich aromatic rings, and the strongly reduced range of aromatic CH signals concurs with the transformation of ArO-Alkyl ether moieties to phenolic Ar-OH moieties. Similarly, deshielded CH moieties have certainly been converted during hydrogenolysis. This is attributed to the removal of neighboring electron-withdrawing groups that decrease the electron density at the nucleus, thereby deshielding the nucleus, which results in a larger chemical shift. Conversely, new signals are observed that are assigned to more-shielded CH moieties. Furthermore, in

the range of methoxy groups, several new signals are observed which are consistent with chemical transformations at the aromatic ring the methoxy groups are attached to. In the aliphatic region, certain signals are transformed, whereas other signals remain nearly unchanged. Noteworthy is the significantly enhanced signal intensity for the methoxy groups in both HSQ NMR spectra compared to the DNP-enhanced solid-state ^{13}C CP-MAS NMR spectrum of the parent kraft lignin. This suggests that lignin fragments with aromatic methoxy moieties have a high propensity to be dissolved in DMSO employed as an NMR solvent. The mostly phenolic hydroxy groups in the lignin oil are not observed in the HSQC NMR spectra. Nevertheless, a broad signal assigned to the proton of the phenolic moieties is prominent at 8.7–8.8 ppm in the ^{1}H-NMR spectra (Figures S2 and S3 for Ru/C and Pt/C, respectively).

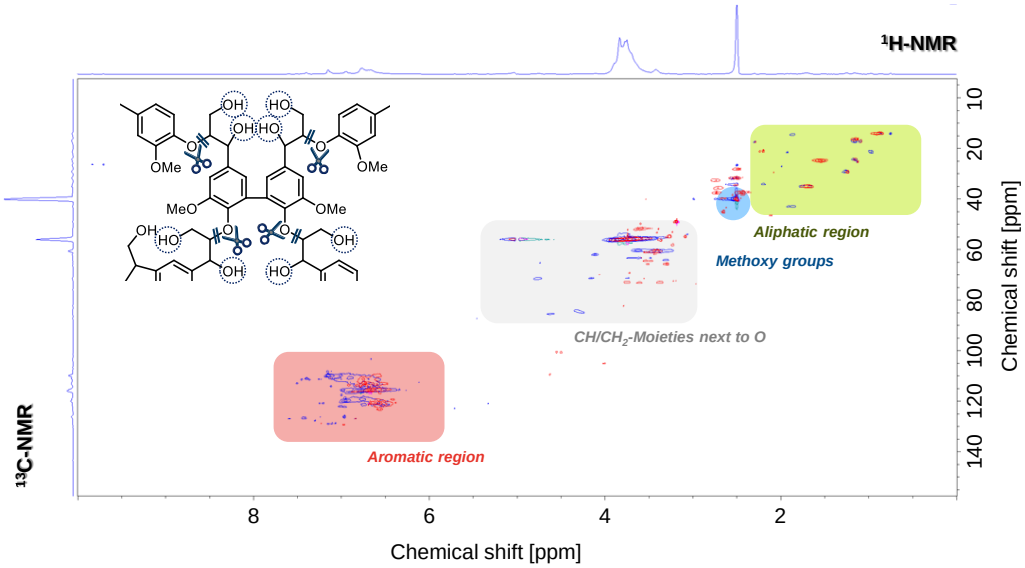

Figure 7. Overlay plot of the HSQC NMR spectra of the parent kraft lignin (blue and green) and the lignin oil (red and pink) obtained by the Ru/C-catalyzed hydrogenolysis of kraft lignin in methanol at supercritical conditions (30 bar initial hydrogen pressure, 131 bar pressure at 250 °C). The insert exemplifies the cleavage of aromatic ether moieties by hydrogenolysis. Bonds that are proposed to be hydrogenolytically cleaved are highlighted with a scissor and the symbol //.

The observed difference in the NMR spectra of the parent kraft lignin and the lignin oil obtained by catalytic hydrogenolysis are fully consistent with cleavage of the ArO-Alkyl ether moieties by hydrogenolysis (Figure 7, insert) and hydrogenation of unsaturated alkenes. The ruthenium-catalyzed hydrogenolysis of the ArO-Alkyl sp^3 C-O bond may proceed through an outer-sphere dihydrogen transfer similar to the mechanism reported for hydroxycyclopentadienyl iridium complexes [51]. In this case, cleavage of the sp^3 C-O bond to phenolic products would take preference over cleavage of the ArO-Alkyl sp^2 C-O bond that gives rise to the corresponding deoxygenized aromatics. Moreover, a retro-aldol pathway could be taken for the hydrogenolytic cleavage of the ArO-Alkyl ether moieties [52]. Noteworthy is the hydroxy group attached to the ß-carbon that may enable this transformation (Figure 7, circles).

3.4. Role of Methanol Solvent in the Hydrogenolysis of Lignin

The solvent methanol plays a key role in the conversion of lignin under our reaction conditions. Several factors may be relevant here:

(i) Of all alcohols, methanol has the highest solubility for hydrogen [53]. Nevertheless, the solubility of hydrogen in methanol (5.21×10^{-5} mol·cm^{-3} at 1.56 MPa and 278 K, [54]) is very low but increases linearly with pressure. High pressure together with conditions close to the supercritical point (vide supra) ensure high availability of hydrogen necessary for efficient hydrogenolysis reactions and avoid potential,

mass transfer limitations from occurring. The rapid saturation of unsaturated entities in the chemical intermediates of lignin degradation, such as aldehyde, keto, and alkene groups, is essential to prevent the repolymerization of lignin fragments and concomitant formation of new hard-to-cleave carbon bonds.

(ii) Through polar interactions and hydrogen bonding, methanol can bind to the ether moieties and hydroxyl groups of lignin, thereby opening the structure of lignin for coordination with the catalyst. The phenolic oxygen atom has a strong propensity as a hydrogen bond acceptor [55] that matches well with the hydrogen bond donor ability of methanol. Furthermore, attractive O-H $\cdots$ π-interactions between the OH group of methanol and the aromatic rings of lignin [56] may contribute to the solvent interactions. Such weak interactions resemble conventional hydrogen bonds (see also [57]) and due to their high number, can contribute substantially to the solvent interactions.

(iii) Likewise, the reaction intermediates and their generated products are stabilized by the solvent methanol through the formation of polar interactions and hydrogen-bonding interactions. In particular, aldehydes and ketones that are formed as reaction intermediates may be converted to the corresponding ortho esters in a reversible fashion. In this way, the keto groups are protected against nucleophilic reactions until they become hydrogenated or undergo hydrogenolysis on the catalyst surface.

(iv) Similarly, the high dipole moment of methanol may lower the energy of polar transition states, thereby enhancing chemical rates. Also, the formation of solvent cages [58], similar to the solvent cages observed for ionic liquids [59], may occur that encapsulate [60] lignin fragments until these are dismantled in further hydrogenolysis reactions.

(v) The high solubility of reaction intermediates and generated products in methanol enhances easy separation from the catalyst surface. Thus, potential catalyst poisoning resulting from the strong coordination of product molecules to the catalyst surface is reduced. Please note that the product molecules may bind strongly in a chelating fashion through several oxygen atoms to the ruthenium atoms exposed at the catalyst surface.

3.5. Chemical Transformations in the Lignin Depolymerization in Methanol

Regarding the chemical transformations that occur in the hydrogenolytic depolymerization of lignin in methanol, we presume that cleavage of ArO-Alkyl ether entities (*vide supra*) is the predominant reaction under our reaction conditions (Scheme 3). Cleavage of the ether bond in the ß position of the aromatic ring readily explains the formation of 4-methylguaiacol (red). Likewise, cleavage of one or two ArO-Alkyl ether bonds leads to the formation of 4-propylguaiacol precursors. The reduction in keto groups, the reductive elimination of aliphatic hydroxy groups on the side chain, and the double bond migration give rise to isoeugenol (see Scheme 2), which is subsequently hydrogenated to 4-propylguaiacol (blue). We presume that there is a mechanism in place that degrades the length of the propyl side chains in a stepwise manner, eventually causing the formation of 4-ethylguaiacol and 4-methylguaiacol from 4-propylguaiacol. Similarly, hydrogenolytic cleavage may explain the formation of 4-substituted 2,6-dimethoxyphenol entities. Side-chain degradation of the 4-propyl-2,6-dimethoxyphenol then leads to 4-ethyl-2,6-dimethoxyphenol (orange). Such a side-chain degradation may occur after the reductive elimination of aliphatic hydroxy groups and double bond migration through reverse hydroformylation with the concomitant release of carbon monoxide (see Scheme 2 for R = methyl, alkyl = ethyl).

In addition, the formation of oligomeric fragments is readily explained by this model. Hydrogenolytic cleavage of aliphatic AlkylO–Alkyl ether bonds under our reaction conditions (absence of base) may be much slower than the cleavage of ArO-Alkyl ether bonds. Also, note that there are no hydroxy groups at the carbon in the ß position that may be necessary for hydrogenolytic cleavage of the ether bonds. Nevertheless, the hydroxy groups would be formed through hydrogenolytic cleavage of the neighboring ArO-Alkyl ether entities. Cleavage of the connecting ArO-Alkyl ether entities generates oligomeric entities

(Scheme 3, purple). Lignin fragments that contain aromatic entities linked by continuous carbon chains (Scheme 3, linkages in bold) appear to remain intact under our reaction conditions giving rise to oligomeric fragments, once all connecting ArO-Alkyl ether entities have been cleaved.

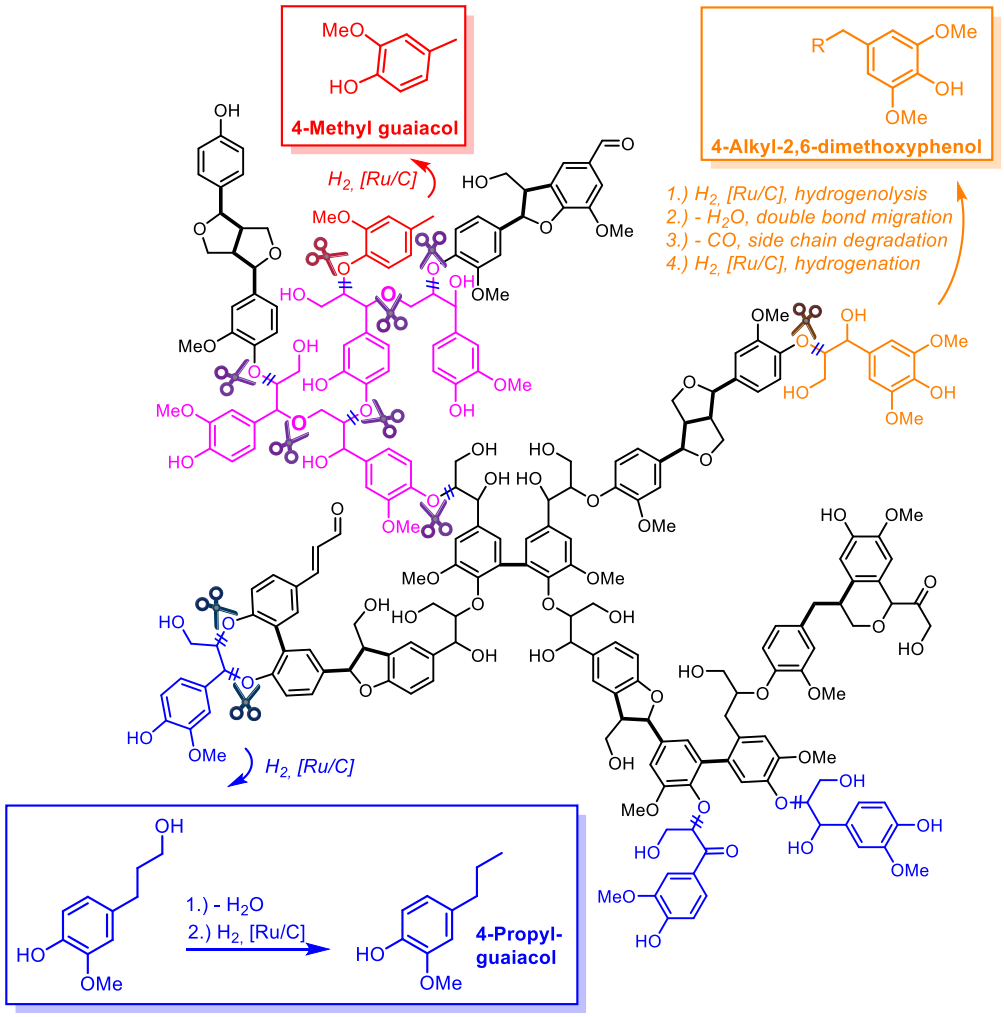

Scheme 3. Proposed cleavage (scissors) of aryl ether bonds explaining the formation of 4-methylguaiacol (red), 4-propylguaiacol (blue), and 4-alkyl-2,6-dimethoxyphenol entities (orange) in the ruthenium-catalyzed hydrogenolysis of kraft lignin. Bonds that are proposed to be hydrogenolytically cleaved are highlighted with the symbol //. Carbon chains linking aromatic entities are highlighted in bold, oligomeric fragments connected through aliphatic ether bonds in purple; simplified structure of lignin, see also [16].

4. Materials and Methods

4.1. Materials

The kraft lignin employed as the feedstock in this study was obtained from Sigma Aldrich (product number 370959, lot number MKCG9481) and was used as supplied. The manufacturer specified the water content at 5%; a weight loss of 3.3, 5.7, 8.5, and 13.4 wt.-% upon heating to 149 °C, 204 °C, 260 °C, and 316 °C, respectively; and a pH-value of 5.5 for a 10 wt.-% aqueous solution at 25 °C. The origin is from softwood. Elemental analysis revealed a composition of C, 61.2; H, 5.388; N, 1.19; S, 1.824; O, 30.398%, which corresponds to an average composition of $C_9H_{9.44}N_{0.15}S_{0.10}O_{3.36}$.

Catalysts and reagents, Ru/C (5 wt.-% Ru, Sigma Aldrich, St. Louis, MO, USA), Pt/C (10 wt.-% Pt; Sigma Aldrich), methanol (UltraPure ≥ 99.9%, VWR, Radnor, PA, USA), and ethanol (absolute, ≥99.8%, Sigma Aldrich) were used as supplied, if not stated otherwise.

4.2. General Procedure

A defined amount of kraft lignin (2.5 g, m^0_{Lignin}) and catalyst ($m_{Catalyst}$), Ru/C (5 wt-%, 2.5 g) or Pt/C (10 wt-%, 1.25 g), were placed into a 300 mL Parr 4560 reactor. The reactor was sealed and flushed three times with nitrogen at 20 bar and then depressurized to ambient pressure. The stirrer was switched on and methanol (100 mL) was added. The reactor was pressurized with hydrogen to 30 bar and sealed. Then, the jacket heating was started at a heating rate of 4 K/min. From the time the reaction mixture had obtained the desired temperature, the reaction mixture was stirred for another 40 min. Then, the reactor was cooled rapidly by immersing the reactor into an ice bath. The pressure was released from the reactor. The product mixture was removed from the reactor and filtered. The volatiles were removed from the filtrate under reduced pressure. A viscous oil was obtained ($m_{Lignin\text{-}oil}$). A portion of the lignin oil was dissolved in methanol and the composition of the mixture was analyzed with a gas chromatograph equipped with a mass sensitive detector (GC-MS) as detailed below. The filter residue was dried at 100 °C for 24 h and weighed ($m_{Filter\ residue}$). Conversion X and lignin-oil yield Y were calculated according to Equations (1) and (2), respectively:

$$X = \frac{m^0_{Lignin} - \left(m_{Filter\ residue} - m_{Catalyst}\right)}{m^0_{Lignin}} \times 100\% \quad (1)$$

$$Y = \frac{m_{Lignin\ oil}}{m^0_{Lignin}} \quad (2)$$

4.3. Procedure Base-Catalyzed Reaction

A defined amount of kraft lignin (10 g, m^0_{Lignin}), NaOH (125 mmol, 5 g) and water (100 mL) was placed into a 300 mL Parr 4560 reactor. The reactor was sealed and flushed three times with nitrogen at 20 bar and then pressurized with nitrogen to 35 bar. The stirrer was switched on and the jacket heating was started at a heating rate of 4 K/min. The reaction mixture was heated to 290 °C for 45 min. Then, the reactor was cooled rapidly by immersing the reactor into an ice bath. The pressure was released from the reactor. The product mixture was removed from the reactor and filtered and washed with water. The filtrate was acidified with aqueous HCl to pH = 1.7 and stirred at 70 °C for 15 min. Afterward, the mixture was filtered and the filtrate was extracted three times with diethyl ether. The combined organic phases were dried over anhydrous $MgSO_4$ and then the volatiles were removed under reduced pressure. Samples for GC measurement were prepared according to the general procedure (*vide supra*).

4.4. Instruments and Analytical Methods

Elemental analyses were performed on a vario MICRO cube from Elementar Analysensysteme GmbH.

GC-MS analyses were performed on an Agilent 7000D Triple Quadrupole GC/MS instrument equipped with an HP5 column. Two sets of calibration mixtures were prepared. For the set of first calibration mixtures, GC vials were charged with benzyl alcohol (25 mg) as the internal standard (t_R 6.343 min) and the calibration compounds 4-methylguaiacol, 4-ethylguaiacol, and 4-propylguaiacol in rising amounts (0, 3, 5, 10, 20, 40, or 75 mg). Methanol was added until the total mass of the mixture was 1 g. The second set of calibration mixtures was prepared in the same way with guaiacol and isoeugenol as the calibration compounds. For analysis of the reaction mixtures, benzyl alcohol (25 mg), lignin oil (75 mg), and methanol (900 mg) were weighed into a GC vial. The products were identified by comparison with mass spectra from the database of the National Institute of Standards and Technology (NIST, [41]).

Guaiacol, t_R 7.374 min; *7.374/z* (%) 125 (5), 124 (70), 110 (7), 109 (100), 108 (6), 95 (2), 82 (7), 81 (85), 79 (3), 77 (7).

4-Methylguaiacol, t_R 9.510 min; *m*/*z* (%) 139 (10), 138 (96), 124 (8), 123 (100), 122 (5), 121 (3), 109 (2), 107 (4), 106 (3), 106 (4).

4-Ethylguaiacol, t_R 11.225 min; *m*/*z* (%) 153 (3), 152 (38), 150 (1), 139 (1), 138 (9), 137 (100), 135 (3), 124 (1), 123 (2), 122 (14).

4-Propylguaiacol, t_R 12.910 min; *m*/*z* (%) 166 (44), 138 (26), 137 (100), 136 (16), 122 (21), 94 (13), 86 (18), 85 (17), 73 (69), 71 (17).

Isoeugenol, t_R 15.787 min; *m*/*z* (%) 165 (10), 164 (100), 163 (13), 162 (1), 150 (6), 149 (50), 147 (5), 146 (2), 139,1 (5), 135 (2).

4-Ethyl-2,6-dimethoxyphenol or isomer, t_R 17.703 min; *m*/*z* (%) 182 (100), 183 (11).

The solid-state NMR spectra were conducted on a Bruker DSX 400 WB spectrometer equipped with a Bruker 263 GHz gyrotron. For DNP, the samples were prepared as follows: 30 mg of sample were impregnated with a solution of 20 µL of water containing 15 mM of AMUPol polarizing agent. About 20 mg of the sample was packed into a 3.2 mm sapphire rotor with a Teflon top insert and a ZrO_2 cap.

The ^{1}H and ^{13}C NMR spectra were recorded on a Bruker AV400 spectrometer. The spectra were analyzed with the software TopSpin 3.2. Deuterated chloroform-d^1 was used as solvent, if not stated otherwise. The ^{1}H NMR spectra were referenced to the chloroform solvent peak at 7.26 ppm. The ^{13}C NMR spectra were referenced to the chloroform solvent peak at 77.16 ppm. For HSQC NMR, the samples were suspended in DMSO-d6. About 83 wt.-% of the sample was dissolved. The insoluble fraction was filtered off and the HSQ NMR spectra of the clear solution were recorded at 400 MHz.

5. Conclusions

The choice of catalyst, solvent effects, and the reaction conditions play central roles in the hydrogenolysis of lignin to mononuclear aromatic compounds. The experimental study showed that methanol is a suitable solvent for the depolymerization of kraft lignin. The reaction conditions around the critical point of methanol are well-suited. The use of Ru/C or Pt/C as a hydrogenolysis catalyst leads to a substantial increase in the yield of mononuclear aromatics. Significantly, their sulfur tolerance makes the catalysts suitable for processing kraft lignin. In parallel to hydrogenolytic cleavage of ArO-Alkyl ether moieties to phenolic Ar-OH moieties, vinylic moieties in isoeugenol, and 4-vinylguaiacol are similarly reduced. This results in an increased yield of 4-propylguaiacol and 4-methylguaiacol. Further investigations could involve convergent synthesis protocols that should generate increased yields of mononuclear aromatics and reduced diversity in the functionality of the aromatic products.

Supplementary Materials: The following supporting information can be downloaded at: https://www.mdpi.com/article/10.3390/catal12060664/s1, Figure S1: Powder XRD measurement of Ru/C, Figure S2: Powder XRD measurement of Pt/C. The red lines indicate the reflexes of cubic Pt as recorded in the Crystallography Open Database (record no. CDO 1011107), Figure S3: Overlay plot of the HSQC NMR spectra of the parent kraft lignin (blue and green) and the lignin oil (red and pink) obtained by the Pt/C catalyzed hydrogenolysis of kraft lignin in methanol at supercritical conditions (30 bar initial hydrogen pressure, 131 bar pressure at 250 °C), Figure S4: ^{1}H and ^{13}C{^{1}H} NMR spectrum of lignin oil obtained by catalytic hydrogenolysis over Ru/C, Figure S5: ^{1}H and ^{13}C{^{1}H} NMR spectrum of lignin oil obtained by catalytic hydrogenolysis over Pt/C.

Author Contributions: Conceptualization, T.E.M.; methodology, D.P. and T.E.M.; software, D.P. and G.B.; validation, D.P.; formal analysis, D.P. and T.E.M.; investigation, D.P. and G.B.; resources, T.E.M.; data curation, D.P. and T.E.M.; writing—original draft preparation, G.B.; writing—review and editing, T.E.M.; visualization, D.P. and T.E.M.; supervision, T.E.M.; project administration, T.E.M.; funding acquisition, T.E.M. All authors have read and agreed to the published version of the manuscript.

Funding: This research was made possible by the state of North Rhine-Westphalia, grant number IRR-2018-1, the Faculty of Mechanical Engineering of Ruhr-Universität Bochum, and RWE Power AG as part of the endowed chair CSC. We acknowledge support from the DFG Open Access Publication Funds of the Ruhr-Universität Bochum.

Data Availability Statement: Not applicable.

Acknowledgments: We gratefully acknowledge the stimulating scientific discussions with Michael Dröscher. We also wish to thank Andrea Krause for experimental support.

Conflicts of Interest: The authors declare no conflict of interest. The funders had no role in the design of the study; in the collection, analyses, or interpretation of data; in the writing of the manuscript, or in the decision to publish the results.

References

1. Tomkins, P.; Müller, T.E. Evaluating the carbon inventory, carbon fluxes and carbon cycles for a long-term sustainable world. *Green Chem.* **2019**, *21*, 3994–4013. [CrossRef]
2. Kätelhön, A.; Meys, R.; Deutz, S.; Suh, S.; Bardow, A. Climate change mitigation potential of carbon capture and utilization in the chemical industry. *Proc. Natl. Acad. Sci. USA* **2019**, *116*, 11187–11194. [CrossRef]
3. Głowacki, E.D.; Voss, G.; Leonat, L.; Irimia-Vladu, M.; Bauer, S.; Sariciftci, N.S. Indigo and Tyrian Purple—From Ancient Natural Dyes to Modern Organic Semiconductors. *Isr. J. Chem.* **2012**, *52*, 540–551. [CrossRef]
4. Sabesan, M.N.; Harper, E.T. Are aromatic residues essential at the "active sites" of peptide hormones? *J. Theor. Biol.* **1980**, *83*, 457–467. [CrossRef]
5. de la Rosa, L.A.; Moreno-Escamilla, J.O.; Rodrigo-García, J.; Alvarez-Parrilla, E. Chapter 12—Phenolic Compounds. In *Postharvest Physiology and Biochemistry of Fruits and Vegetables*; Yahia, E.M., Ed.; Woodhead Publishing: Sawston, UK, 2019; pp. 253–271.
6. Calvo-Flores, F.G.; Dobado, J.A.; Isac-García, J.; Martín-MartíNez, F.J. *Lignin and Lignans as Renewable Raw Materials: Chemistry, Technology and Applications*; John Wiley & Sons, Ltd.: Hoboken, NJ, USA, 2015.
7. Cheng, K.; Hagiopol, C. *Natural Polyphenols from Wood, Tannin and Lignin—An Industrial Perspective*; Elsevier: Amsterdam, The Netherlands, 2021.
8. L'udmila, H.; Michal, J.; Andrea, Š.; Aleš, H. Lignin, potential products and their market value. *Wood Res.* **2015**, *60*, 973–986.
9. Bajwa, D.S.; Pourhashem, G.; Ullah, A.H.; Bajwa, S.G. A concise review of current lignin production, applications, products and their environmental impact. *Ind. Crops Prod.* **2019**, *139*, 111526. [CrossRef]
10. Gou, M.; Ran, X.; Martin, D.W.; Liu, C.-J. The scaffold proteins of lignin biosynthetic cytochrome P450 enzymes. *Nat. Plants* **2018**, *4*, 299–310. [CrossRef]
11. Hu, J.; Zhang, Q.; Lee, D.-J. Kraft lignin biorefinery: A perspective. *Bioresour. Technol.* **2018**, *247*, 1181–1183. [CrossRef]
12. *Lignin, Biosynthesis and Transformation for Industrial Applications*; Springer International Publishing: Cham, Switzerland, 2020; 298p.
13. Production of Biofuels and Chemicals from Lignin. In *Biofuels and Biorefineries*; Springer: Singapore, 2016; Volume XV, 435p.
14. del Río, J.C.; Rencoret, J.; Gutiérrez, A.; Elder, T.; Kim, H.; Ralph, J. Lignin Monomers from beyond the Canonical Monolignol Biosynthetic Pathway: Another Brick in the Wall. *ACS Sustain. Chem. Eng.* **2020**, *8*, 4997–5012. [CrossRef]
15. Lignin Chemistry. In *Topics in Current Chemistry Collections (TCCC)*; Springer: Berlin/Heidelberg, Germany, 2020; Volume VI, 271p.
16. Balakshin, M.; Capanema, E.A.; Zhu, X.; Sulaeva, I.; Potthast, A.; Rosenau, T.; Rojas, O.J. Spruce milled wood lignin: Linear, branched or cross-linked? *Green Chem.* **2020**, *22*, 3985–4001. [CrossRef]
17. Rinaldi, R.; Jastrzebski, R.; Clough, M.T.; Ralph, J.; Kennema, M.; Bruijnincx, P.C.A.; Weckhuysen, B.M. Paving the Way for Lignin Valorisation: Recent Advances in Bioengineering, Biorefining and Catalysis. *Angew. Chem. Int. Ed.* **2016**, *55*, 8164–8215. [CrossRef]
18. Azadi, P.; Inderwildi, O.R.; Farnood, R.; King, D.A. Liquid fuels, hydrogen and chemicals from lignin: A critical review. *Renew. Sustain. Energy Rev.* **2013**, *21*, 506–523. [CrossRef]
19. Cheremisinoff, N.P.; Rosenfeld, P.E. Chapter 6—Sources of air emissions from pulp and paper mills. In *Handbook of Pollution Prevention and Cleaner Production*; Cheremisinoff, N.P., Rosenfeld, P.E., Eds.; William Andrew Publishing: Oxford, UK, 2010; pp. 179–259.
20. Chakar, F.S.; Ragauskas, A.J. Review of current and future softwood kraft lignin process chemistry. *Ind. Crops Prod.* **2004**, *20*, 131–141. [CrossRef]
21. Gruber, E. *Grundlagen der Zellstofftechnologie: Vorlesungsskriptum zum Lehrgang "Papiertechnik"*; Duale Hochschule Baden-Württemberg Karlsruhe: Karlsruhe, Germany, 2011.
22. Tomani, P.E.R. The lignoboost process. *Cellul. Chem. Technol.* **2010**, *44*, 53–58.
23. Vishtal, A.; Kraslawski, A. Challenges in industrial applications of technical lignins. *Bioresour. Technol.* **2011**, *6*, 3547–3568. [CrossRef]
24. Zhang, C.; Wang, F. Catalytic Lignin Depolymerization to Aromatic Chemicals. *Acc. Chem. Res.* **2020**, *53*, 470–484. [CrossRef]
25. Wang, H.; Tucker, M.; Ji, Y. Recent Development in Chemical Depolymerization of Lignin: A Review. *J. Appl. Chem.* **2013**, *2013*, 838645. [CrossRef]
26. Roberts, V.M.; Stein, V.; Reiner, T.; Lemonidou , A.; Li, X.; Lercher, J.A. Towards Quantitative Catalytic Lignin Depolymerization. *Chem. Eur. J.* **2011**, *17*, 5939–5948. [CrossRef]
27. Müller, T. Hydrogenation and Hydrogenolysis with Ruthenium Catalysts and Application to Biomass Conversion. In *Ruthenium: An Element Loved by Researchers*; Ishida, H., Ed.; IntechOpen: London, UK, 2021.
28. Kristianto, I.; Limarta, S.O.; Lee, H.; Ha, J.-M.; Suh, D.J.; Jae, J. Effective depolymerization of concentrated acid hydrolysis lignin using a carbon-supported ruthenium catalyst in ethanol/formic acid media. *Bioresour. Technol.* **2017**, *234*, 424–431. [CrossRef]

29. Yan, N.; Zhao, C.; Dyson, P.J.; Wang, C.; Liu, L.-T.; Kou, Y. Selective Degradation of Wood Lignin over Noble-Metal Catalysts in a Two-Step Process. *ChemSusChem* **2008**, *1*, 626–629. [CrossRef]
30. Chio, C.; Sain, M.; Qin, W. Lignin utilization: A review of lignin depolymerization from various aspects. *Renew. Sustain. Energy Rev.* **2019**, *107*, 232–249. [CrossRef]
31. Zhao, C.; Kou, Y.; Lemonidou, A.A.; Li, X.; Lercher, J.A. Highly Selective Catalytic Conversion of Phenolic Bio-Oil to Alkanes. *Angew. Chem. Int. Ed.* **2009**, *48*, 3987–3990. [CrossRef]
32. Dong, L.; Yin, L.-L.; Xia, Q.; Liu, X.; Gong, X.-Q.; Wang, Y. Size-dependent catalytic performance of ruthenium nanoparticles in the hydrogenolysis of a β-O-4 lignin model compound. *Catal. Sci. Technol.* **2018**, *8*, 735–745. [CrossRef]
33. Zakzeski, J.; Jongerius, A.L.; Bruijnincx, P.C.A.; Weckhuysen, B.M. Catalytic Lignin Valorization Process for the Production of Aromatic Chemicals and Hydrogen. *ChemSusChem* **2012**, *5*, 1602–1609. [CrossRef]
34. Shu, R.; Long, J.; Xu, Y.; Ma, L.; Zhang, Q.; Wang, T.; Wang, C.; Yuan, Z.; Wu, Q. Investigation on the structural effect of lignin during the hydrogenolysis process. *Bioresour. Technol.* **2016**, *200*, 14–22. [CrossRef]
35. Xu, W.; Miller, S.J.; Agrawal, P.K.; Jones, C.W. Depolymerization and Hydrodeoxygenation of Switchgrass Lignin with Formic Acid. *ChemSusChem* **2012**, *5*, 667–675. [CrossRef]
36. Ma, R.; Hao, W.; Ma, X.; Tian, Y.; Li, Y. Catalytic Ethanolysis of Kraft Lignin into High-Value Small-Molecular Chemicals over a Nanostructured α-Molybdenum Carbide Catalyst. *Angew. Chem. Int. Ed.* **2014**, *126*, 7438–7443. [CrossRef]
37. Baerns, M.; Behr, A.; Brehm, A.; Gmehling, J.; Hinrichsen, K.-O.; Hofmann, H.; Onken, U.; Palkovits, R.; Renken, A. *Technische Chemie*, 2nd ed.; Springer: Berlin/Heidelberg, Germany, 2014; 762p.
38. Kouris, P.D.; van Osch, D.J.G.P.; Cremers, G.J.W.; Boot, M.D.; Hensen, E.J.M. Mild thermolytic solvolysis of technical lignins in polar organic solvents to a crude lignin oil. Sustain. *Energy Fuels* **2020**, *4*, 6212–6226.
39. Girard, E.; Tassaing, T.; Marty, J.-D.; Destarac, M. Structure–Property Relationships in CO_2-philic (Co)polymers: Phase Behavior, Self-Assembly, and Stabilization of Water/CO_2 Emulsions. *Chem. Rev.* **2016**, *116*, 4125–4169. [CrossRef]
40. Aymonier, C.; Philippot, G.; Erriguible, A.; Marre, S. Playing with chemistry in supercritical solvents and the associated technologies for advanced materials by design. *J. Supercrit. Fluids* **2018**, *134*, 184–196. [CrossRef]
41. Linstrom, P.J. NIST Standard Reference Database Number 69. In *NIST Chemistry WebBook*; U.S. Department of Commerce: Washington, DC, USA, 2022.
42. Shu, R.; Zhang, Q.; Ma, L.; Xu, Y.; Chen, P.; Wang, C.; Wang, T. Insight into the solvent, temperature and time effects on the hydrogenolysis of hydrolyzed lignin. *Bioresour. Technol.* **2016**, *221*, 568–575. [CrossRef]
43. Wang, J.; Li, W.; Wang, H.; Ma, Q.; Li, S.; Chang, H.-m.; Jameel, H. Liquefaction of kraft lignin by hydrocracking with simultaneous use of a novel dual acid-base catalyst and a hydrogenation catalyst. *Bioresour. Technol.* **2017**, *243*, 100–106. [CrossRef]
44. Brand, S.; Susanti, R.F.; Kim, S.K.; Lee, H.-S.; Kim, J.; Sang, B.-I. Supercritical ethanol as an enhanced medium for lignocellulosic biomass liquefaction: Influence of physical process parameters. *Energy* **2013**, *59*, 173–182. [CrossRef]
45. Lee, H.-S.; Jae, J.; Ha, J.-M.; Suh, D.J. Hydro- and solvothermolysis of kraft lignin for maximizing production of monomeric aromatic chemicals. *Bioresour. Technol.* **2016**, *203*, 142–149. [CrossRef]
46. Cheng, S.; D'cruz, I.; Wang, M.; Leitch, M.; Xu, C. Highly Efficient Liquefaction of Woody Biomass in Hot-Compressed Alcohol−Water Co-solvents. *Energy Fuels* **2010**, *24*, 4659–4667. [CrossRef]
47. Kim, J.-Y.; Oh, S.; Hwang, H.; Cho, T.-S.; Choi, I.-G.; Choi, J.W. Effects of various reaction parameters on solvolytical depolymerization of lignin in sub- and supercritical ethanol. *Chemosphere* **2013**, *93*, 1755–1764. [CrossRef]
48. Cheng, S.; Wilks, C.; Yuan, Z.; Leitch, M.; Xu, C. Hydrothermal degradation of alkali lignin to bio-phenolic compounds in sub/supercritical ethanol and water–ethanol co-solvent. Polym. *Degrad. Stab.* **2012**, *97*, 839–848. [CrossRef]
49. Nguyen, T.D.H.; Maschietti, M.; Belkheiri, T.; Åmand, L.-E.; Theliander, H.; Vamling, L.; Olausson, L.; Andersson, S.-I. Catalytic depolymerisation and conversion of Kraft lignin into liquid products using near-critical water. *J. Supercrit. Fluids* **2014**, *86*, 67–75. [CrossRef]
50. Ye, Y.; Zhang, Y.; Fan, J.; Chang, J. Selective production of 4-ethylphenolics from lignin via mild hydrogenolysis. *Bioresour. Technol.* **2012**, *118*, 648–651. [CrossRef]
51. Kusumoto, S.; Nozaki, K. Direct and selective hydrogenolysis of arenols and aryl methyl ethers. *Nat. Commun.* **2015**, *6*, 6296. [CrossRef]
52. Shen, X.; Zhang, C.; Han, B.; Wang, F. Catalytic self-transfer hydrogenolysis of lignin with endogenous hydrogen: Road to the carbon-neutral future. *Chem. Soc. Rev.* **2022**, *51*, 1608–1628. [CrossRef]
53. Katayama, T.; Nitta, T. Solubilities of hydrogen and nitrogen in alcohols and n-hexane. *J. Chem. Eng. Data* **1976**, *21*, 194–196. [CrossRef]
54. Gemo, N.; Biasi, P.; Salmi, T.O.; Canu, P. H_2 solubility in methanol in the presence of CO_2 and O_2. *J. Chem. Thermodyn.* **2012**, *54*, 1–9. [CrossRef]
55. Beller, M.; Riermeier, T.H.; Mägerlein, W.; Müller, T.E.; Scherer, W. Chemistry of chelate-stabilized aryloxopalladium(II) complexes: Syntheses, X-ray crystal structures and formation of C≡H ... O hydrogen-bonds. *Polyhedron* **1998**, *17*, 1165–1176. [CrossRef]
56. Desiraju, G.R.; Steiner, T. *The Weak Hydrogen Bond: In Structural Chemistry and Biology International Union of Crystallography Monographs on Crystallography*; Oxford University Press: Oxford, UK, 2001; 528p.
57. Müller, T.E.; Mingos, D.M.P.; Williams, D.J. T-shaped intermolecular CH$\cdots\pi$(C≡C) interactions in chloroform solvates of gold(I) ethyne complexes. *J. Chem. Soc. Chem. Commun.* **1994**, 1787–1788. [CrossRef]

58. Li, Y.; Ruan, W. From Solvent Cage to Molecular Cage. *Univ. Chem.* **2012**, *27*, 76–81. [CrossRef]
59. Sievers, C.; Jimenez, O.; Müller, T.E.; Steuernagel, S.; Lercher, J.A. Formation of Solvent Cages around Organometallic Complexes in Thin Films of Supported Ionic Liquid. *J. Am. Chem. Soc.* **2006**, *128*, 13990–13991. [CrossRef]
60. Tsuji, Y.; Richard, J.P. Reactions of ion-pair intermediates of solvolysis. *Chem. Rec.* **2005**, *5*, 94–106. [CrossRef]